

Phononic properties of a periodic nanostructure including vacuum gap in the presence of effective interatomic interactions

Leila Ghaderipoor,^{1,*} Mohammad Mardaani,^{1,2,†} Ehsan Amooghorban^{1,2,‡} and Hassan Rabani^{1,2,§}

¹*Department of Physics, Faculty of Science, Shahrekord University, P. O. Box 115, Shahrekord, Iran*

²*Nanotechnology Research Center, Shahrekord University, P.O. Box 8818634141, Shahrekord, Iran*



(Received 3 May 2021; accepted 2 September 2021; published 16 September 2021)

Using the harmonic approximation and Green's function technique, we investigate the contribution of phonons to heat transport across a narrow vacuum gap by an extended mass-spring chain model. We base the investigation on the van Beest–Kramer–van Santen potential that applies to two cases of simple and alternating mass systems at a finite temperature. Employing this model, we show that in specific values of interaction strengths, incoming phonon frequency, and gap distance, the phonon transmission across the vacuum gap can be improved. Finally, the thermal conductance of the system is computed as a function of interaction strength, gap distance, and temperature. These calculations reveal a suitable fitting function that can provide valuable insight into determining the internal interaction strengths from this quantity or controlling it by variation of the gap distance.

DOI: [10.1103/PhysRevE.104.034121](https://doi.org/10.1103/PhysRevE.104.034121)

I. INTRODUCTION

The heat transfer between two bodies with different temperatures placed in close proximity has attracted a great deal of attention in recent years because of the drastically enhanced heat flux between them. It is well known that the heat energy exchanged between bodies at enormous distances follows the Stefan-Boltzmann law [1]; however, this law is no longer valid when the distance between them becomes smaller than the thermal wavelength. In this near-field region, the radiative heat transfer is dominant due to the tunneling of evanescent waves. It has been shown both theoretically [2–7] and experimentally [8–12] that the near-field heat flux can increase by several orders of magnitude compared to the conventional black-body radiation.

When the separation distance between the two bodies lies in the scale of their lattice constant, besides this near-field radiative heat transfer, the thermal conduction mediated by phonons becomes dominant in the heat transfer mechanisms also [13–16]. Some recent investigations, using different techniques and considering effects such as tunneling of acoustic phonons [17–29], have shown that several orders of magnitude of near-field radiative heat flux can further enhance the heat transfer at distances of a few nanometers. This enhanced heat transfer has attracted much attention because of the wide potential applications in thermal microscopy, imaging [30–33], energy harvesting [34–36], and nanofabrication devices [3,5]. Sellan *et al.* [17], based on lattice dynamics calculations and Landauer theory [37], has investigated the heat transfer via acoustic phonons between two silicon sur-

faces and found that the heat flux would be four orders of magnitude larger than the near-field heat transfer. However, they only considered the interaction between surface atoms via their electron clouds and ignored the long-range van der Waals (vdW) interaction between the bodies. Altfeder *et al.* [18], using ultrahigh vacuum inelastic scanning tunneling microscopy, have reported a field-induced phonon tunneling mechanism. They showed that the heat transfer due to the phonon tunneling can be much larger than the value predicted by the black-body radiation. Ezzahri and Joulain [13] demonstrated that vdW and Casimir forces as new mechanisms can also assist phonon tunneling in narrow vacuum gaps. They found that for highly doped silicon, phonon-mediated heat transfer prevails over radiative transfer. But they only considered the ballistic transport of phonons across the gap and did not explain the role of different modes of elastic waves that can excite in such medium. Chiloyan *et al.* [19] followed the method introduced by Ezzahri *et al.* and modeled the Coulombic interaction of atoms across the vacuum gap with a springlike behavior to calculate phonon transmission. They found that the contribution of low frequency acoustic phonons is important in subnanometer gaps. However, the sinusoidal variation of the surface topology of the solids because of the presence of phonons was not considered. Pendry *et al.* [26] considered these effects in the calculation of the transmission coefficient of phonons when two identical objects are separated by small spacings. Later, Sasihithlu *et al.* [20] extended this work to objects of different materials. Xiong *et al.* [14], using the phononic nonequilibrium Green's function technique, investigated the heat transfer between two silica clusters. Within the investigated gap distances, they identified three typical regions with different heat transfer behaviors and emphasized the importance of acoustic phonon tunneling in heat transmission.

The contribution of phonons to heat transfer can be mediated by interatomic potentials such as van Beest, Kramer,

*ghaderipoor.l@stu.sku.ac.ir

†mohammad-m@sku.ac.ir

‡ehsan.amooghorban@sku.ac.ir

§rabani-h@sku.ac.ir

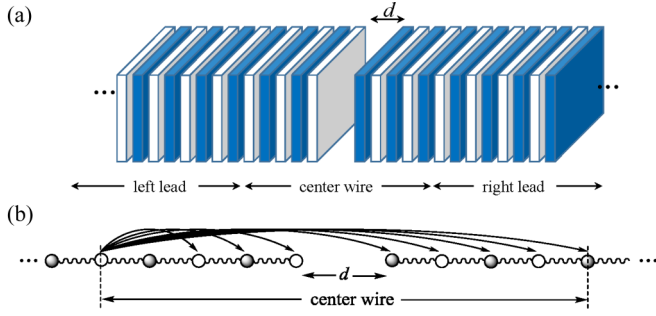


FIG. 1. (a) Two semi-infinite bodies containing alternating crystal planes with different masses separated by a narrow vacuum gap. The structure is divided into three parts: center wire, and left and right leads. The crystal planes only in the center part are assumed to have equally positive and negative charges, alternatively. (b) A scheme of the extended mass-spring model with the masses and springs that correspond to masses and the constant forces of interplane bonds, respectively. In fact, the center wire is supposed to be ionic including long-range Coulomb interaction. Here, the arrows show the corresponding force constants.

and van Santen (BKS) [26,38]. Generally, the phonons cannot propagate in the bulk vacuum [17], while, thanks to this potential, they can tunnel across a nanometer vacuum gap from one surface to another. Such a mechanism can be interpreted by different microscopic theories such as the *ab initio* approach, scattering boundary method, and Green's function technique [39–41].

With attention to the importance of this enhanced energy transfer for both the fundamental interest and practical value, we follow the work done on silica clusters by Xiong *et al.* [14] and present a simple model to study the phonon tunneling between two semi-infinite bodies separated by a narrow vacuum gap based on the BKS potential and using the harmonic approximation and Green's function technique. The BKS potential includes long-range Coulomb, vdW, and short-range repulsive interactions. We see that this model as an alternative superlattice, which is reduced to the corresponding mass-spring chains, analytically enables us to compute the self-energies as functions of incoming phonon frequency and force constants of springs in leads and contacts. Given this and taking into account the simplicity of our model, an increase in the speed of numerical calculations occurs, and we can get an estimation and overview of the problem in a short time with a small effort. In this manner, we can easily calculate phonon transmission and the thermal conductance for two cases of simple and alternating mass chains. This also provides the ability to understand the nature and the strength of the interaction from the behavior of thermal conductance.

This paper is organized as follows. In Sec. II, we propose a mass-spring harmonic model to study heat transfer between two semi-infinite bodies. In Sec. III, the numerical results are discussed. We finish the paper with conclusions in Sec. IV.

II. MODEL AND FORMALISM

We consider a setup consisting of two semi-infinite bodies separated by a narrow vacuum gap with distance d [Fig. 1(a)] and propose an extended mass-spring model to simulate the

contribution of phonons to heat transfer, as displayed in Fig. 1(b). Indeed, each atomic layer is supposed to be a mass and the atomic force between them is followed by Hooke's law. We define the center wire (W) by $N/2$ masses at the left and the same numbers at the right of the gap (N is the number of masses in this part). The other masses belong to two semi-infinite left (L) and right (R) leads. Let us assume that the layers in the center wire and leads have alternative masses m and M , while their charges are supposed to be, alternatively, q and $-q$ in the center wire, and zero in leads. The force constant between the nearest-neighbor masses, C_0 , exists in the entire system except in the vacuum gap. In the center wire, there is also the force constant between the next-neighbor (i th and j th) masses, C_{ij} , derived by the BKS potential as

$$\frac{C_{ij}}{C_0} = \frac{\lambda_C (-1)^{i+j}}{|i-j|^3} + \lambda_E e^{-|i-j|} - \frac{\lambda_V}{(i-j)^8}, \quad (1)$$

where i and j are both in the same nongap regions. Similarly, this formula can calculate the force constants by replacing $j \rightarrow d/a + j$ in the denominators of Eq. (1) when i and j are in the different regions around the gap. Here, a is the lattice constant and d is the gap width (concerning the distance between the nearest masses). To distinguish these two cases, we use the notation C_{ij}^d for the latter case. Here, λ_C , λ_E , and λ_V are the strengths of the Coulomb, exponential, and vdW potentials, respectively. The first term in Eq. (1) refers to the Coulomb interaction and the others originate from the Pauli exclusion principle and the vdW energy. To define the vacuum gap, the nearest-neighbor force constant C_0 between the masses $N/2$ and $N/2 + 1$ is taken at zero. With these definitions and under the assumption of the harmonic approximation, the elements of the dynamic matrix of this mass-spring system, \mathbf{C} , can be written as

$$(\mathbf{C})_{i,i} = C_0(2 - \delta_{i, N/2}) + \sum_{j=1}^{N/2} C_{ij} + \sum_{j=N/2+1}^N C_{ij}^d, \quad (2a)$$

$$(\mathbf{C})_{N+1-i, N+1-i} = (\mathbf{C})_{i,i}, \text{ where } i \leq N/2 \text{ and } j \neq i, \quad (2b)$$

$$(\mathbf{C})_{i,i+1} = C_0(1 - \delta_{i, N/2}) + C_{i,i+1}, \quad (2c)$$

$$(\mathbf{C})_{i,j} = C_{ij}, \quad i = 1, \dots, \frac{N}{2} - 2;$$

$$j = i + 2, \dots, \frac{N}{2},$$

$$\text{and } i = \frac{N}{2} + 1, \dots, N - 2; j = i + 2, \dots, N, \quad (2c)$$

$$(\mathbf{C})_{i,j} = C_{ij}^d, \quad i = 1, \dots, \frac{N}{2}; \quad j = \frac{N}{2} + 1, \dots, N,$$

$$\text{and } j \neq i + 1, \quad (2d)$$

$$(\mathbf{C})_{i,j} = (\mathbf{C})_{j,i}. \quad (2e)$$

Therefore, the phononic Green's function \mathbf{G} of the center wire in the presence of leads is obtained by

$$\mathbf{G} = \frac{1}{\mathbf{M}\omega^2 - \mathbf{C} - \boldsymbol{\Sigma}}, \quad (3)$$

where \mathbf{M} stands for a diagonal mass matrix with alternative elements m and M ; ω is the input phonon frequency; and $\boldsymbol{\Sigma}$ is the phononic self-energy diagonal matrix whose first and last elements only, corresponding to the left (Σ_L) and right (Σ_R)

self-energies, are nonzero. They read [42–44]

$$\Sigma_L = \Sigma_R = \frac{C_0(2 - \omega^2/\omega_0^2)}{1 + \xi + \sqrt{\xi^2 - 1}}, \quad (4)$$

where

$$\xi = \left(1 - \frac{\omega^2}{2\omega_0^2}\right) \left(2 - \frac{M\omega^2}{m\omega_0^2}\right) - 1.$$

Here, $\omega_0 = \sqrt{C_0/m}$ is the natural phonon frequency of the system with the value of the order of $\sim 10^{12}$ - 10^{13} Hz. By substituting Eqs. (2) and (4) into Eq. (3), the elements of the inverse Green's function matrix are obtained. Therefore, by the inversion of this matrix, we can calculate the phonon transmission coefficient as a function of phonon frequency, $T(\omega)$, according to the following formula [37]:

$$T(\omega) = 4 \text{Im} \Sigma_L \text{Im} \Sigma_R |G_{1,N}|^2, \quad (5)$$

where $G_{1,N}$ is the leftmost entry of the center part Green's function. We also introduce the local phonon density of states at the sites around the vacuum gap $N/2$ and $N/2 + 1$ as [42]

$$\text{LDOS} = -\frac{2\omega}{\pi} \text{Im}(G_{N/2,N/2} + G_{N/2+1,N/2+1}). \quad (6)$$

Moreover, the thermal conductance can be computed by [45]

$$\kappa = \frac{k_B \beta^2 \hbar^2}{2\pi} \int_0^{\omega_c} T(\omega) \frac{\omega^2 e^{\beta \hbar \omega}}{(e^{\beta \hbar \omega} - 1)^2} d\omega, \quad (7)$$

where ω_c is the cutoff phonon frequency, \hbar is the reduced Planck's constant, and $\beta = 1/k_B T$, in which T is the temperature and k_B is the Boltzmann constant. Now, we are in a position to investigate the phonon transport properties of two semi-infinite bodies.

III. RESULTS

In this section, we examine the model for a lengthy polar mass-spring nanowire that includes two types of alternating positive and negative ions with different masses (AB chain), i.e., an existing subnanometer vacuum gap in the nanowire. Three types of interactions, i.e., the Coulomb, the vdW, and the short-range repulsive interactions, can influence the thermal properties of the system. Here, we calculate the phonon transmission coefficient of the system as a function of phonon frequency, the gap space distance, and the strength of these interactions. The thermal conductance is computed in terms of temperature, the gap space distance, and the strength of these interactions. We report our results in dimensionless quantities. For example, the phonon frequency, temperature, and gap distance are expressed in units of ω_0 , $\hbar\omega_0/k_B$, and a , respectively. To make the effect of leads and contacts in the model under study negligible, the number of ions in the center part of the chain, N , should be chosen as a big enough number. A part of the wire where there are interactions defines the center wire. According to our calculations, $N = 120$ is an optimum number which we use in drawing the following plots. Before describing the results, it is better to discuss the typical strength values of two main interactions, namely, λ_C and λ_V . Assume the energy scale ratio of the vdW and Coulomb potentials to be ε . Therefore, the second derivative of this potential gives

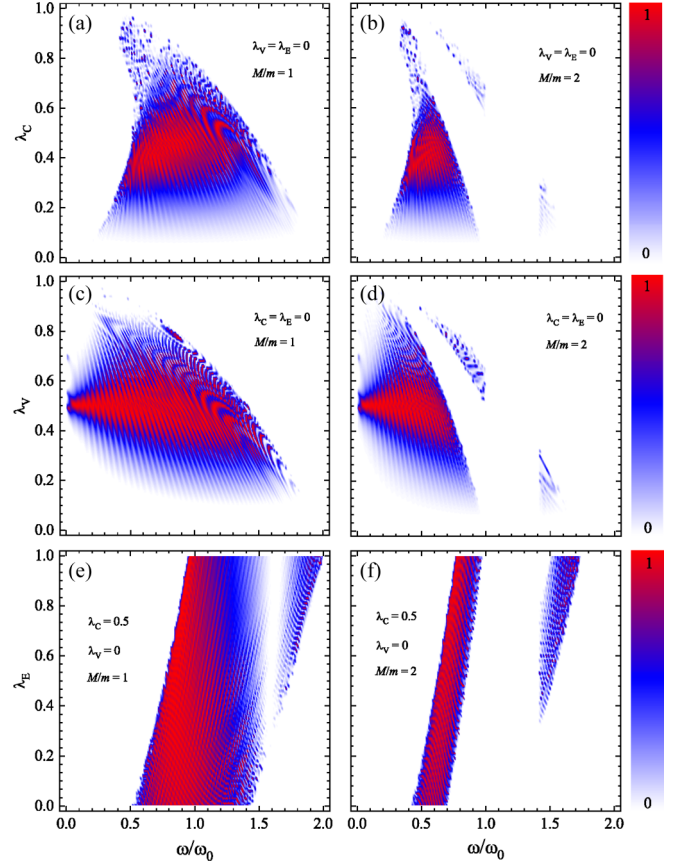


FIG. 2. Phonon transmission coefficient as a function of phonon frequency and the strength of (a), (b) Coulomb, (c), (d) vdW, and (e), (f) short-range repulsive interactions for a polar mass-spring nanowire with gap space distance of $d/a = 1$. Two different values for the mass ratio of alternating masses are chosen: (a), (c), (e) $M/m = 1$ and (b), (d), (f) $= 2$. The other interactions are absent in each pair of plots except in (e) and (f) where we take $\lambda_C = 0.5$.

the ratio of $\lambda_V/\lambda_C = 21\varepsilon$. Since the typical values of ε lie in the range ~ 0.002 - 0.05 , we have $\lambda_V/\lambda_C \simeq 0.04 \sim 1$ [46]. Regarding λ_E , if we take its value in the magnitude of λ_C , then the short-range potential is expanded to one unit cell.

In Fig. 2, we present the phonon transmission coefficient of the system as a function of phonon frequency and the strength of the Coulomb [Figs. 2(a) and 2(b)], vdW [Figs. 2(c) and 2(d)], and short-range repulsive interactions [Figs. 2(e) and 2(f)] for the two cases of $M = m$ (simple chain) and $M = 2m$ (AB chain). In each pair of the Figs. 2(a), 2(b), 2(c), and 2(d), the other interactions are absent, while in Figs. 2(e) and 2(f), there is no vdW interaction and the strength of the Coulomb interaction is fixed at $\lambda_C = 0.5$. In this figure, we set the gap space distance in the system equal to the lattice constant, $d = a$. The dispersion relation of the mass-spring leads, i.e., $\omega = 2\omega_0 |\sin ka/2|$ wherein k is the phonon wave number, determines the range of ω as $[0, 2\omega_0]$. The range of $\lambda_{C(V,E)}$ is chosen as $[0, 1]$ in which the value of 1 corresponds to the strength of an interaction creating a force constant equal to C_0 . According to the counterplots of Figs. 2(a) and 2(b), despite the existence of a vacuum gap, $T(\omega, \lambda_C)$ can be nonzero due to the long-range nature of the Coulomb

interaction. The maximum value of $T(\omega, \lambda_C)$ occurs at the middle values of ω and λ_C . The frequency range for nonzero transmission is decreasing by increasing λ_C . Therefore, there are some regions where the Coulomb interaction improves the phonon transmission in the system. Comparing Fig. 2(a) with Fig. 2(b), we can see that the effect of the Coulomb interaction on phonon transfer is more observable in the simple mass-spring chain compared to the *AB* one. Moreover, it is seen that in Figs. 2(a) and 2(b), the nonzero transmission has been extended in the frequency window of $[0,2]$ for the simple chain, while for the *AB* case, it has a notable value just in the range $[0,1]$. We mention here that the frequency gap in the *AB* model for $M/m = 2$ lies in $[1,2]$ [47]. We can also observe this aspect in other figures related to the phonon transmission coefficient. We find that only when the vdW interaction exists in the chain [see Figs. 2(c) and 2(d)], there is a nonzero transmission in a range at the phonon frequency edge compared to the Coulomb case. Thus, for intermediate values of λ_V , even in very low frequencies, the phonon can transfer through the vacuum gap. Also, at most frequencies, the phonon conductance turns on at the larger value of λ_V [Figs. 2(c) and 2(d)] with respect to the value of λ_C [Figs. 2(a) and 2(b)]. Furthermore, in the higher ω region, $T(\omega, \lambda_V)$ exists at lower λ_V . For the short-range repulsive interaction, there is no notable phonon transfer through the system. Therefore, we examine this effect together with a constant strength of the Coulomb interaction, $\lambda_C = 0.5$, in Figs. 2(e) and 2(f). It is seen that by increasing the value of λ_E , the frequency range that the phonon can transfer through the system shifts to higher frequencies. The maximum value of $T(\omega, \lambda_E)$ is almost independent of the value of λ_E . A gap region has been created at frequencies around $\omega = 1.6\omega_0$ in the mass-spring simple chain in Fig. 2(e). This gap has been extended for the *AB* chain in Fig. 2(f) by adding to its intrinsic frequency gap. The existence of semi-infinite phononic leads limits the frequency of the incident phonon in the common band frequencies. In addition, the frequency channels (or quasilevels) in the center wire are determined by parameters such as interaction strengths, distance gap, and so on. Therefore, the incident phonons coming from leads with frequencies corresponding to channel frequencies of the center part can easily transmit through the system and the transmission coefficient takes its maximum value. Whatever the number of these frequency channels lying in the common range of band frequencies of the leads decreases, the value of the transmission coefficient decreases. Therefore, the variation of the values of interaction strengths shifts the frequency channels “in” or “out” of the band frequency of leads, resulting, respectively, in increasing or decreasing the transmission coefficient. Since the peaks of the total density of states (DOS) of the system correspond to the conductance channels and the contribution of local DOS of vibrating atoms around the vacuum gap, which are more affected by the creation of new channels, we present the local DOS (LDOS) corresponding to the transmission of Figs. 2(a)–2(d) in Fig. 3. We observe that by increasing the Coulomb and vdW interaction strengths, some new peaks appear in the LDOS(ω) curve.

Figure 4 displays the phonon transmission coefficient as a function of phonon frequency and gap space distance when the strength values of the interactions are fixed for the two

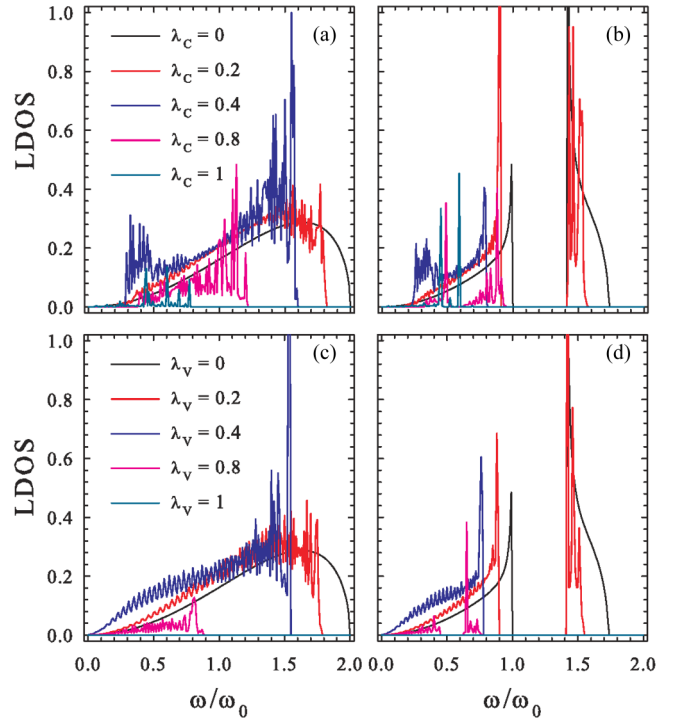


FIG. 3. The local phonon density of states in arbitrary units at the sites around the vacuum gap as a function of phonon frequency for some different strength values of (a), (b) Coulomb and (c), (d) vdW interaction, and the polar mass-spring nanowire whose transmission is plotted in Fig. 2. Here, the mass ratio of alternating masses is chosen: (a), (c) $M/m = 1$ and (b), (d) $= 2$. In each plot, the other interactions are absent.

cases of simple [Figs. 4(a), 4(c), and 4(e)] and *AB* [Figs. 4(b), 4(d), and 4(f)] chains. It is evident that by increasing the value of d , the phonon transmission frequency tends to zero. In Figs. 4(a) and 4(b), only the Coulomb interaction with strength $\lambda_C = 0.5$ is presented. In this case, only in a narrow window of frequencies is the phonon allowed to transfer through the system. This window is narrower in the *AB* chain than in the simple one, which means that the ratio of alternating masses, M/m , would determine the allowed width of transferring phonon frequency band. The next plots, Figs. 4(c) and 4(d), respectively, belong to the simple and the *AB* chains in the presence of the vdW interaction ($\lambda_V = 0.5$) when other interactions are absent. Here, despite Figs. 4(a) and 4(b), the allowed frequency windows begin from zero for the values of d near a , although the beginning frequency moves to the higher frequencies with increasing d . However, the values of the cutoff frequencies in Figs. 4(c) and 4(d) correspond to the ones in Figs. 4(a) and 4(b), respectively. As explained before, to understand the effect of the short-range repulsive interaction, we have to consider the Coulomb interaction also. Figures 4(e) and 4(f) are plotted for the parameters $\lambda_E = 0.5$ and $\lambda_C = 0.5$. As expected, the general aspect of the transmission spectra is determined by the Coulomb interaction and therefore these plots are very similar to Figs. 4(a) and 4(b). However, a shift in the frequency window can be seen when both interactions are present. For the simple chain [Fig. 4(e)], the short-range repulsive interaction creates a new narrow

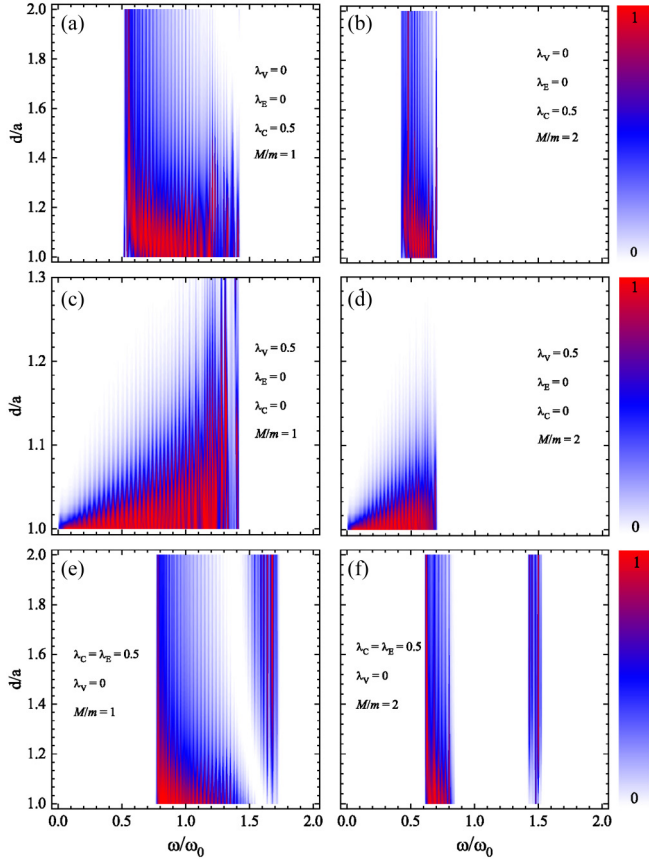


FIG. 4. Phonon transmission coefficient as a function of phonon frequency and gap space distance for a polar mass-spring nanowire. The strength values of the Coulomb, vdW and short-range repulsive interactions are fixed as follows: (a), (b) $\lambda_C = 0.5$, $\lambda_V = \lambda_E = 0$, (c), (d) $\lambda_V = 0.5$, $\lambda_C = \lambda_E = 0$, and (e), (f) $\lambda_C = \lambda_E = 0.5$, $\lambda_V = 0$. Two different values for the mass ratio of alternating masses are chosen: (a), (c), (e) $M/m = 1$ and (b), (d), (f) = 2.

frequency gap at the end of the allowed phonon frequency window which, by increasing d , shifts its position to the lower frequencies. Similarly, in the *AB* chain [Fig. 4(f)], a narrow new frequency window opens at higher frequencies. In Figs. 4(e) and 4(f), we see that at high frequencies, it can even enhance the phonon transmission by the increase of the vacuum gap distance. It seems that some narrow frequency channels are slowly created at high frequencies with increasing the distance gap. In our model, we take a lengthy interacting system between two phononic leads. When a frequency channel of the center subsystem lies in the range of band frequency of the leads, the resonance phonon transmission mechanism can occur. The creation of narrow frequency channels can be attributed to the long-range aspect of the Coulomb and the vdW interactions. We present, in Fig. 5, the local phonon density of states as a function of phonon frequency corresponding to the transmission of Figs. 4(e) and 4(f), for some different values of gap space distance. As we mentioned before, the arising values of the LDOS in a frequency range corresponds to the creation of the new channel in that domain. Indeed, some new peaks are observed in LDOS at larger values of d .

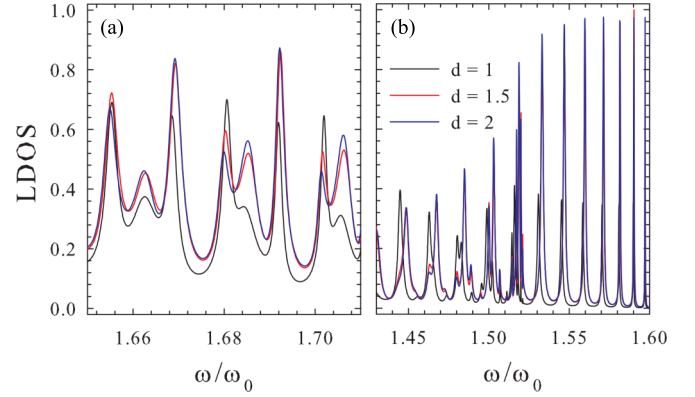


FIG. 5. The local phonon density of states in arbitrary units at the sites around the vacuum gap as a function of phonon frequency for some different strength values of gap space distance for the polar mass-spring nanowire whose transmission is presented in Figs. 4(e) and 4(f). The value of M/m is (a) 1 and (b) 2. Note that here the vdW interaction is absent. Also, the range of frequency axes in each plot is chosen in a small domain in which the transmission is ascendant vs d in Fig. 4.

Figure 6 shows the phononic thermal conductance as a function of temperature and one of the interaction strengths for the simple [Figs. 6(a), 6(c), and 6(e)] and *AB* Figs. 6(b), 6(d), and 6(f) mass-spring chains including a vacuum gap. We express this quantity in terms of units of $k_B\omega_0/2\pi$. We observe that there is a correspondence between the thermal conductance and transmission plots at low temperatures (see Fig. 2). Therefore, according to Eq. (7), the value of the transmission coefficient directly influences the thermal conductance. In general, the value of κ for the *AB* mass-spring chain is smaller than for the simple one. In the absence of other interactions and at a finite temperature, the best values of the Coulomb interaction strength that creates the maximum thermal conductance lies in $\sim[0.3, 0.5]$ [for Fig. 6(a)] and $\sim[0.3, 0.4]$ [for Fig. 6(b)]. This scenario works for Figs. 6(c) and 6(d) where only the vdW interaction exists. But here, at low temperatures and intermediate values of λ_V , the thermal conductance also has nonzero values. In Figs. 6(e) and 6(f), κ is plotted as a function of temperature and short-range repulsive interaction when the value of λ_C is taken to be 0.5. It is seen that at high temperatures, the maximum thermal conductance occurs at small (large) values of λ_E for the simple (*AB*) chain. This is due to the existence of a wider frequency gap in the phonon conductance spectra of the *AB* chain, which causes the role of acoustic phonons to fade.

The effect of gap space distance d on the thermal conductance is considered in Fig. 7. Generally, by increasing the temperature, κ increases, and by raising the value of d , a decreasing behavior is observed. However, the insets in Figs. 7(a) and 7(b) show that at an optimum gap space distance, the thermal conductance takes a maximum value when the Coulomb interaction prevails in the system.

In the end, we extract a suitable fitting function for thermal conductance as a function of the Coulomb interaction strength (in the range of $0 < \lambda_C < 1$) and gap distance (in the range of $1 < d/a < 2$) in Figs. 6(a) and 6(b) and Figs. 7(a) and 7(b) as

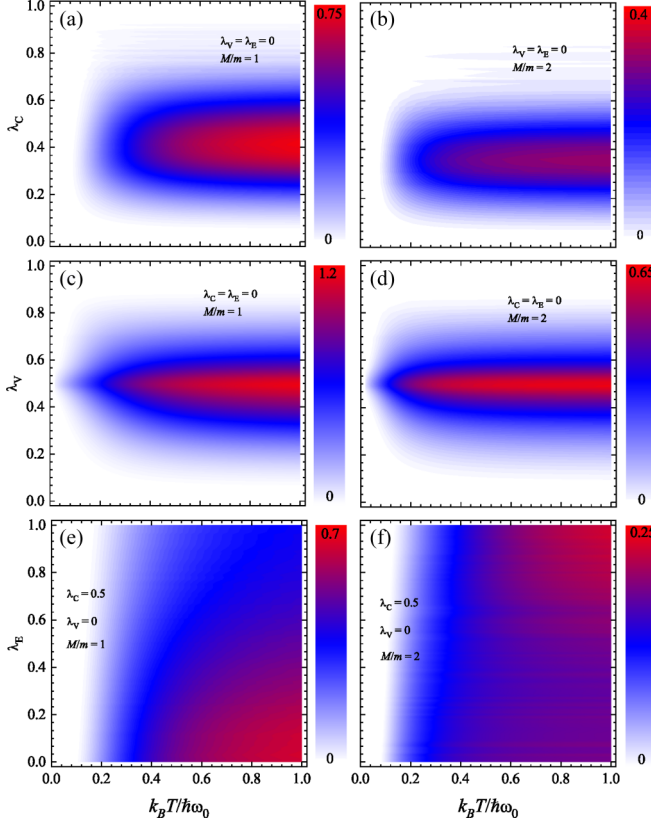


FIG. 6. Thermal conductance as a function of temperature and the strength of (a), (b) Coulomb, (c), (d) vdW, and (e), (f) short-range repulsive interactions for a polar mass-spring nanowire with gap space distance of $d/a = 1$. Two different values for the mass ratio of alternating masses are chosen: (a), (c), (e) $M/m = 1$ and (b), (d), (f) $M/m = 2$. The other interactions are absent in each pair of plots, except in (e), (f) where we take $\lambda_C = 0.5$.

follows:

$$\frac{\kappa(\lambda_C, d)}{\kappa_{\max}} = \left[1 + \alpha \left(1 + \frac{d_0}{d} - 2 \frac{d_0^2}{d^2} \right) \right] \exp \left[-\frac{(\lambda_C - \lambda_0)^2}{2\sigma^2} \right],$$

where κ_{\max} , α , d_0 , λ_0 , and σ are the maximum of the thermal conductance, fitting parameter, optimum space gap, optimum strength of the Coulomb interaction, and standard deviation, respectively. All of these parameters are temperature dependent except d_0 and λ_0 , which are almost temperature independent. Moreover, the κ_{\max} in terms of temperature can fit on a Hill function. It is an important result because an observable parameter such as the thermal conductance can be related to the interaction strength by this relation. In other words, the thermal conductance measurements can provide an estimate of the Coulomb interaction strength. This relation enables us to control and optimize this quantity by variation of the gap space.

IV. CONCLUSION

We theoretically studied the phonon tunneling across an alternating mass-spring chain including a vacuum gap in the presence of the Coulomb, vdW, or short-range repulsive interactions. We considered two cases of simple and *AB* chains,

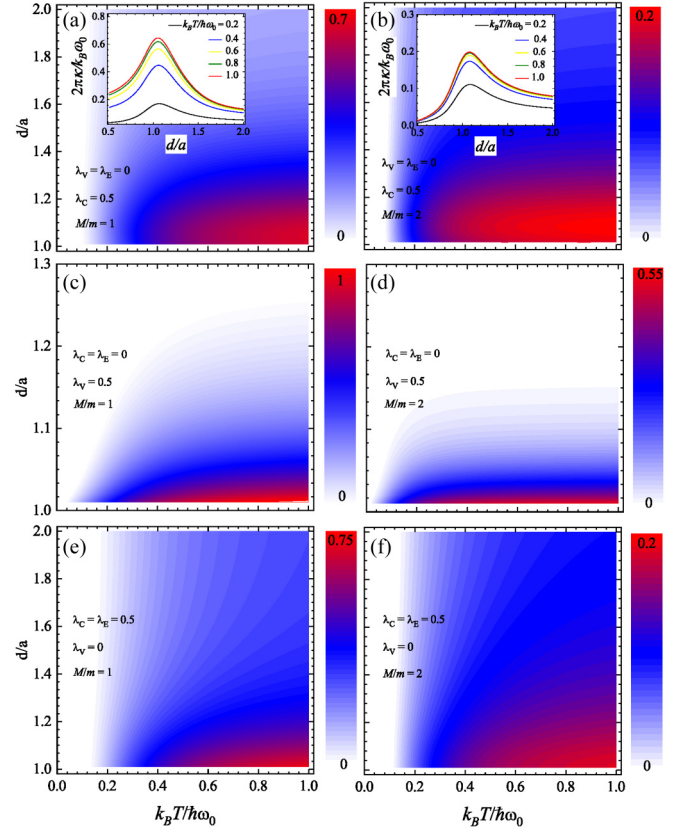


FIG. 7. Thermal conductance as a function of temperature and gap space distance for a polar mass-spring nanowire. The strength values of the Coulomb, vdW, and short-range repulsive interactions are fixed as follows: (a), (b) $\lambda_C = 0.5$, $\lambda_V = \lambda_E = 0$, (c), (d) $\lambda_V = 0.5$, $\lambda_C = \lambda_E = 0$, and (e), (f) $\lambda_C = \lambda_E = 0.5$, $\lambda_V = 0$. Two different values for the mass ratio of alternating masses are chosen: (a), (c), (e) $M/m = 1$ and (b), (d), (f) $M/m = 2$. The insets in (a) and (b) show the corresponding thermal conductivities as functions of gap space distance at several fixed values of temperature.

respectively, corresponding to intrinsic gapless and gapped systems. We based the presented model on the harmonic approximation and Green's function technique. In this way, we obtained the phonon self-energy for the *AB* mass-spring chain and then calculated the phonon transmission coefficient as a function of phonon frequency, the strengths of interactions, and the gap space distance. We numerically investigated the thermal conductance and found its dependence on temperature, the strengths of interactions, and the gap space distance.

The results show that the phonon can transfer through the system in a determined frequency window and in a special range value of the strength of the Coulomb and vdW interactions. Especially for a weak Coulomb interaction and at low phonon frequencies, the phonon transmission coefficient has no significant value, while at the intermediate strength of the vdW interaction, it takes nonzero values at low phonon frequencies. Considering the short-range repulsive interaction with the Coulomb one, the transferring region shifts into higher frequencies by creating a narrow frequency gap inside. The increase of gap space distance decreases the phonon tunneling, as expected. Only when the vdW interaction works

is this decrease faster for low phonon frequencies. It may be possible to create a narrow allowed frequency band by selecting specific values of interaction strength and the gap space distance in the AB mass-spring chain. The thermal conductance of the simple chain is larger than the AB one with the same parameters. At low temperatures and for both cases, it vanishes except for intermediate values of the vdW interaction strength that show a small value. There are optimal

values of strengths for the Coulomb and the vdW interactions in which the thermal conductance behaves like a Gaussian function. The measurement of the phononic contribution of thermal conductance can provide useful information about the strengths of internal interactions existing between ions in the system. This model can also be used for superlattice nanostructures to develop thermal switching and other applications.

-
- [1] R. H. Dicke and J. P. Wittke, *Introduction to Quantum Mechanics* (Addison-Wesley, Reading, MA, 1960).
- [2] D. Polder and M. Van Hove, *Phys. Rev. B* **4**, 3303 (1971).
- [3] J. B. Pendry, *J. Phys.: Condens. Matter* **11**, 6621 (1999).
- [4] K. Joulain, J. P. Mulet, F. Marquier, R. Carminati, and J. J. Greffet, *Surf. Sci. Rep.* **57**, 59 (2005).
- [5] A. I. Volokitin and B. N. J. Persson, *Phys. Rev. B* **63**, 205404 (2001).
- [6] A. I. Volokitin and B. N. J. Persson, *Rev. Mod. Phys.* **79**, 1291 (2007).
- [7] S. Bayati, E. Amooghorban, and A. Mahdifar, *Iran. J. Phys. Res.* **18**, 263 (2018).
- [8] S. Shen, A. Narayanaswamy, and G. Chen, *Nano Lett.* **9**, 2909 (2009).
- [9] E. Rousseau, A. Siria, G. Jourdan, S. Volz, F. Comin, J. Chevrier, and J. J. Greffet, *Nat. Photon.* **3**, 514 (2009).
- [10] B. Song, A. Fiorino, E. Meyhofer, and P. Reddy, *AIP Adv.* **5**, 053503 (2015).
- [11] L. Cui, W. Jeong, V. Fernandez-Hurtado, J. Feist, F. J. Garcia-Vidal, J. C. Cuevas, E. Meyhofer, and P. Reddy, *Nat. Commun.* **8**, 1 (2017).
- [12] K. Kim, B. Song, V. Fernandez-Hurtado, W. Lee, W. Jeong, L. Cui, D. Thompson, J. Feist, M. T. Homer Reid, F. J. Garcia-Vidal, J. C. Cuevas, E. Meyhofer, and P. Reddy, *Nature (London)* **528**, 387 (2015).
- [13] Y. Ezzahri and K. Joulain, *Phys. Rev. B* **90**, 115433 (2014).
- [14] S. Xiong, K. Yang, Y. A. Kosevich, Y. Chalopin, R. D'Ágosta, P. Cortona, and S. Volz, *Phys. Rev. Lett.* **112**, 114301 (2014).
- [15] K. Sasihithlu, *Nature (London)* **576**, 216 (2019).
- [16] K. Kloppstech, N. Konne, S. A. Biehs, A. W. Rodriguez, L. Worbes, D. Hellmann, and A. Kittel, *Nat. Commun.* **8**, 14475 (2017).
- [17] D. P. Sellan, E. S. Landry, K. Sasihithlu, A. Narayanaswamy, A. J. H. McGaughey, and C. H. Amon, *Phys. Rev. B* **85**, 024118 (2012).
- [18] I. Altfeder, A. A. Voevodin, and A. K. Roy, *Phys. Rev. Lett.* **105**, 166101 (2010).
- [19] V. Chiloyan, J. Garg, K. Esfarjani, and G. Chen, *Nat. Commun.* **6**, 6755 (2015).
- [20] K. Sasihithlu, J. B. Pendry, and R. V. Craster, *Z. Naturforsch.* **72**, 181 (2017).
- [21] A. I. Volokitin, *JETP Lett.* **109**, 749 (2019).
- [22] A. I. Volokitin, *J. Phys.: Condens. Matter* **32**, 215001 (2020).
- [23] A. I. Volokitin and B. N. J. Persson, *J. Phys.: Condens. Matter* **32**, 255301 (2020).
- [24] A. I. Volokitin, *Phys. Rev. B* **103**, L041403 (2021).
- [25] B. N. J. Persson, A. I. Volokitin, and H. Ueba, *J. Phys.: Condens. Matter* **23**, 045009 (2011).
- [26] J. B. Pendry, K. Sasihithlu, and R. V. Craster, *Phys. Rev. B* **94**, 075414 (2016).
- [27] B. V. Budaev and D. B. Bogy, *Appl. Phys. Lett.* **99**, 053109 (2011).
- [28] Z. Y. Ong, Y. Cai, and G. Zhang, *Phys. Rev. B* **94**, 165427 (2016).
- [29] M. Prunnila and J. Meltaus, *Phys. Rev. Lett.* **105**, 125501 (2010).
- [30] Y. D. Wilde, F. Formanek, R. Carminati, B. Gralak, P. A. Lemoine, K. Joulain, J. P. Mulet, Y. Chen, and J. J. Greffet, *Nature (London)* **444**, 740 (2006).
- [31] A. Kittel, W. Muller-Hirsch, J. Parisi, S. A. Biehs, D. Reddig, and M. Holthaus, *Phys. Rev. Lett.* **95**, 224301 (2005).
- [32] A. Kittel, U. F. Wischnath, J. Welker, O. Huth, F. Ruetting, and S. A. Biehs, *Appl. Phys. Lett.* **93**, 193109 (2008).
- [33] F. Huth, M. Schnell, J. Wittborn, N. Ocelic, and R. Hillenbrand, *Nat. Mater.* **10**, 352 (2011).
- [34] M. D. Whale and E. G. Cravalho, *IEEE Trans. Energy Convers.* **17**, 130 (2002).
- [35] S. Basu, Y. B. Chen, and Z. M. Zhang, *Intl. J. Energy Res.* **31**, 689 (2007).
- [36] J. Fang, H. Frederich, and L. Pilon, *J. Heat Transfer* **132**, 092701 (2010).
- [37] S. Datta, *Electronic Transport in Mesoscopic Systems* (Cambridge University Press, Cambridge, 1997).
- [38] B. W. H. van Beest, G. J. Kramer, and R. A. van Santen, *Phys. Rev. Lett.* **64**, 1955 (1990).
- [39] Z. Tian, K. Esfarjani, and G. Chen, *Phys. Rev. B* **86**, 235304 (2012).
- [40] L. Zhang, P. Keblinski, J. S. Wang, and B. Li, *Phys. Rev. B* **83**, 064303 (2011).
- [41] N. Mingo, Green's function methods for phonon transport through nanocontacts, in *Thermal Nanosystems and Nanomaterials*, edited by S. Volz (Springer, Berlin, 2009), Chap. 3.
- [42] M. Mardaani and H. Rabani, *Solid State Commun.* **151**, 311 (2011).
- [43] M. J. Farsani, H. Rabani, and M. Mardaani, *J. Magn. Magn. Mater.* **465**, 270 (2018).
- [44] H. Rabani and M. Mardaani, *Physica E* **67**, 112 (2015).
- [45] A. Chaudhuri, A. Kundu, D. Roy, A. Dhar, J. L. Lebowitz, and H. Spohn, *Phys. Rev. B* **81**, 064301 (2010).
- [46] J. Lv, M. Bai, W. Cui, and X. Li, *Nanoscale Res. Lett.* **6**, 200 (2011).
- [47] G. Grosso and G. P. Paravicini, *Solid State Physics* (Academic Press, San Diego, CA, 2000).